JOURNAL OF VIROLOGY, Nov. 1996, p. 7974–7983 Vol. 70, No. 11
0022-538X/96/$04.00+0

Genetic Map of the Calicivirus Rabbit Hemorrhagic Disease Virus as Deduced from In Vitro Translation Studies

CHRISTOPH WIRBLICH,† HEINZ-JÜRGEN THIEL,‡ AND GREGOR MEYERS*

Federal Research Centre for Virus Diseases of Animals, 72001 Tübingen, Germany

Received 26 February 1996/Accepted 25 July 1996

The 7.5-kb plus-stranded genomic RNA of rabbit hemorrhagic disease virus contains two open reading frames of 7 kb (ORF1) and 351 nucleotides (ORF2) that cover nearly 99% of the genome. The aim of the present study was to identify the proteins encoded in these open reading frames. To this end, a panel of region-specific antisera was generated by immunization of rabbits with bacterially expressed fusion proteins that encompass in total 95% of the ORF1 polyprotein and almost the complete ORF2 polypeptide. The antisera were used to analyze the in vitro translation products of purified virion RNA of rabbit hemorrhagic disease virus. Our studies show that the N-terminal half of the ORF1 polyprotein is proteolytically cleaved to yield three nonstructural proteins of 16, 23, and 37 kDa (p16, p23, and p37, respectively). In addition, a cleavage product of 41 kDa which is composed of VPg and a putative nonstructural protein of approximately 30 kDa was identified. Together with the results of previous studies which identified a trypsin-like cysteine protease (TCP) of 15 kDa, a putative RNA polymerase (pol) of 58 kDa, and the major capsid protein VP60, our data establish the following gene order in ORF1: NH_2-p16-p23-p37 (helicase)-p30-VPg-TCP-pol-VP60-COOH. Immunoblot analyses showed that a minor structural protein of 10 kDa is encoded in ORF2. The data provide the first complete genetic map of a calicivirus. The map reveals a remarkable similarity between caliciviruses and picornaviruses with regard to the number and order of the genes that encode the nonstructural proteins.

The genome of rabbit hemorrhagic disease virus (RHDV), a recently identified member of the family *Caliciviridae* (10, 38, 40, 51), consists of a single plus-stranded RNA of 7,437 nucleotides that has VPg attached covalently to the 5′ end and is polyadenylated at the 3′ end. In addition to the genomic RNA, RHDV produces a subgenomic RNA of 2.2 kb that covers the 3′ third of the genome. Both the genomic and the subgenomic RNAs are packaged in nonenveloped icosahedral capsids that consist of the major structural protein VP60 (31, 32). Sequence analysis of the RHDV genome revealed an open reading frame of 7 kb (ORF1) that encodes a hypothetical polyprotein of 257 kDa. The extreme 3′ region of the RHDV genome contains a second open reading frame, of 351 nucleotides (ORF2), that overlaps ORF1 by several nucleotides and encodes a hypothetical polypeptide of 12.7 kDa. As shown by sequence comparison, the ORF1 polyprotein contains a putative RNA helicase and an RNA polymerase that are homologous to the 2C and 3D proteins of picornaviruses, respectively (31). A trypsin-like cysteine protease (TCP) of caliciviruses that is similar to the 2A and 3C proteases of picornaviruses has been identified recently (5, 54). This protease is located in the central part of the ORF1 polyprotein upstream of the putative RNA polymerase and the major capsid protein; the latter covers the C-terminal part of the ORF1 polyprotein. A similar genome organization has been reported for feline calicivirus (FCV) and two human caliciviruses, Norwalk virus and Southampton virus (7, 22, 27, 36, 37). These viruses, however, differ from RHDV in having two open reading frames of approximately 5.2 and 2 kb that encode the putative nonstructural proteins and the major capsid protein, respectively. A third open reading frame, homologous to ORF2 of RHDV, is present in the 3′ region of the genome (7, 8, 22, 27, 37).

Previous studies have shown that RHDV expresses two capsid protein species that probably differ by only two amino acids at their amino termini (5, 39, 54). The larger capsid protein, which constitutes the major structural protein in mature virions, is generated by translation of the subgenomic RNA, while the minor derivative is produced by translation of the genomic RNA and subsequent proteolytic processing at an EG dipeptide at the polymerase-capsid protein boundary. The latter cleavage occurs 2 amino acids downstream of the N-terminal methionine of the major capsid protein species and is carried out by the TCP encoded in the central part of ORF1. The TCP also exhibits self-cleavage at its N- and C-terminal boundaries. In a recent study the ORF1 polyprotein was found to be cleaved into four primary processing products, p80, p43, p73, and VP60; VP60 represents the viral capsid protein (1). The 80-kDa protein (p80) contains the 2C-like protein, while p73 encompasses the 3C-like protease and the putative polymerase.

In the present paper we report the generation of a panel of region-specific antisera that are directed against different parts of the ORF1 polyprotein and the ORF2 polypeptide. The antisera were used to study the proteolytic processing of the ORF1 polyprotein in rabbit reticulocyte lysates and to analyze the protein composition of purified virions. The results of these studies provide a complete genetic map of RHDV that assigns all of the proteins identified so far by in vitro translation, expression in bacteria, and analysis of RHDV virions to their coding sequences in the genome.

MATERIALS AND METHODS

Plasmid construction and expression in *Escherichia coli*. The pEX-34 vectors have been described previously (52, 54). Standard cloning procedures were used to construct the expression plasmids. The relevant features of the plasmids are

* Corresponding author. Mailing address: Department of Clinical Virology, Federal Research Centre for Virus Diseases of Animals, P.O. Box 1149, D-72001 Tübingen, Germany. Fax: 49 7071-967305. Electronic mail address: gregor.meyers@tue.bfav.de.

† Present address: Department of Neurology, University of Tübingen, D-72076 Tübingen, Germany.

‡ Present address: Institute of Virology, University of Giessen, D-35392 Giessen, Germany.

TABLE 1. Expression of RHDV cDNA fragments in *E. coli*

Construct	Serum	cDNA insert[a]			Amino acids[b]		Molecular mass (kDa)[c]		Vector/restriction site(s)[d]
		Nucleotides	Restriction sites	Amino acids	RHDV	Total	Predicted	Observed	
pEX-A	A	33–918	*Bgl*I-*Nhe*I	9–303	295	431	48.4	48	A/*Bam*HI
pEX-B	B	33–344	*Bgl*I-*Nar*I	9–112	104	224	25.0	26	A/*Bam*HI
pEX-C	C	343–705	*Nar*I-*Sty*I	112–232	121	242	27.1	31	A/*Eco*RI, *Bam*HI
pEX-D	D	702–918	*Sty*I-*Nhe*I	232–303	72	203	22.8	23	B/*Eco*RI
pEX-E	E	1186–2113	*Kpn*I-*Sac*I	393–702	310	435	48	49	A/*Eco*RI
pEX-F	F	2118–3080	*Sac*I-*Eco*RI	704–1023	320	456	51	52	B/*Eco*RI
pEX-G	G	2118–2634	*Sac*I-*Bsp*HI	704–875	172	292	33.3	31	B/*Eco*RI
pEX-H	H	2631–3080	*Bsp*HI-*Eco*RI	875–1023	149	285	31.4	32	B/*Eco*RI
pEX-I	I	3077–3517	*Eco*RI-*Kpn*I	1023–1170	148	276	31.1	31	B/*Eco*RI, *Bam*HI
pEX-J	J	3522–4004	*Kpn*I-*Hin*dIII	1172–1332	161	296	32.9	33	A/*Eco*RI
pEX-K	K	4001–5189	*Hin*dIII-*Xho*I	1332–1727	396	506	56.6	55	B/*Bam*HI, *Pst*I
pEX-L	L	4001–5398	*Hin*dIII-*Bam*HI	1332–1796	465	601	67.1	66	B/*Bam*HI
pEX-M	M	5395–7047	*Bam*HI-*Bam*HI	1796–2344	549	653	69.2	72	B/*Bam*HI
pEX-N	N	7044–7437	*Eco*RI-*Eco*RI	7′–117′	111	210	23	25	B/*Eco*RI
pEX-Q		33–1181	*Bgl*I-*Kpn*I	9–390	382	504			A/*Bam*HI
pEX-R		343–1181	*Nar*I-*Kpn*I	112–390	279	395			A/*Eco*RI, *Bam*HI
pEX-S		702–1181	*Sty*I-*Kpn*I	232–390	159	275			B/*Eco*RI, *Bam*HI
pEX-T		916–1181	*Nhe*I-*Kpn*I	303–390	88	204			A/*Eco*RI, *Bam*HI

[a] Indicated are the nucleotide positions (numbered from the 5′ end of the RHDV genomic RNA) and the corresponding amino acids of the ORF1 or ORF2 (pEX-N) protein (numbered from the first methionine in ORF1 or ORF2). Except for constructs pEX-M and pEX-N, protruding ends were treated with Klenow polymerase to produce blunt ends.

[b] Indicated are the number of amino acids encoded in the RHDV cDNA fragments and the total number of amino acids of the fusion proteins.

[c] Predicted molecular mass indicates the size of the fusion proteins calculated from the amino acid sequence. Observed molecular mass indicates the apparent sizes (by SDS-PAGE analysis) of the fusion proteins. Expression of plasmids pEX-Q, pEX-R, pEX-S, and pEX-T did not yield detectable amounts of the expected fusion proteins.

[d] Indicated are the expression vectors pEX34A and pEX34B (A and B, respectively) and the restriction sites used to insert the cDNA fragments (see footnote *a*).

described in Table 1. Expression of the recombinant plasmids in *E. coli*, purification of the fusion proteins, and immunization of rabbits were carried out as previously described (53, 54).

Virus purification and RNA isolation. Rabbits experimentally infected with RHDV were sacrificed in a moribund state or shortly postmortem. The livers of the animals were removed, dissected into small pieces, and homogenized in phosphate-buffered saline (PBS) at 0°C. Large debris was removed by centrifugation in a JA 10 rotor (Beckman) for 20 min at 9,000 rpm (14,300 × *g*). The clarified supernatant was then transferred in 38-ml thin-walled centrifuge tubes (28 ml per tube), underlaid with 8 ml of 30% (wt/vol) sucrose in PBS, and centrifuged for 2.5 h at 25,000 rpm (112,000 × *g*) in a TST28 rotor (Kontron). The supernatant was removed, and the pelleted material was resuspended in PBS. For Western blot (immunoblot) analysis of viral particles, the suspension was further purified as described below. For RNA isolation, the virus suspension was treated as follows. The resuspended material was extracted several times with Freon 113. To effect phase separation, the mixture was centrifuged for 5 min at 1,000 × *g*. Viral particles in the aqueous phases were collected by centrifugation for 1.5 h at 40,000 rpm (287,000 × *g*) in a TST41 rotor (Kontron). The virions were resuspended in 2 ml of RNA lysis mix (4 M guanidine thiocyanate, 0.5% sarcosyl, 25 mM lithium citrate, 0.1 M β-mercaptoethanol), and the lysate was layered on a 2-ml cushion of 5.7 M CsCl–5 mM EDTA–10 mM Tris (pH 7.5) in a 5-ml tube and centrifuged at 36,000 rpm (164,000 × *g*) in a TST55 rotor for at least 18 h at 20°C. The pelleted RNA was dissolved in diethylpyrocarbonate (DEPC)-treated water, precipitated with ethanol, and finally dissolved in DEPC-treated water.

Iodination of VPg. One microgram of RHDV RNA was used as the starting material for protein labeling with $Na^{125}I$ by the chloramine-T method (17). After completion of the labeling, the RNA was degraded with RNase as described before (32).

Western blot analysis of viral particles. The first steps of virus purification were carried out as described above. After the virus particles were pelleted through a 30% sucrose cushion, the particles were resuspended in PBS and layered on top of a CsCl step gradient consisting of 5 ml of a CsCl solution with a density of 1.65 g/ml and 5 ml of a CsCl solution with a density of 1.28 g/ml in PBS in a TST28 centrifuge bottle. The step gradient was centrifuged for 3 h at 22,000 rpm (87,000 × *g*) in a TST28 rotor at 20°C. After centrifugation, the tubes were punctured at the interface of the two CsCl solutions, and the virus particles were removed, dialyzed against PBS, and finally boiled in protein sample buffer. Western blot analysis was then carried out as described previously (53).

In vitro translation and immunoprecipitation. One microgram of RHDV RNA was heat denatured at 65°C for 5 min in a total volume of 10 μl, chilled on ice, and used as a template for in vitro translation in 35 μl of nuclease-treated rabbit reticulocyte lysate (RRL) (Promega) as suggested by the supplier. [^{35}S]methionine (Amersham, Braunschweig, Germany; 1,000 μCi/mmol) was used at a concentration of 1 μCi/μl to label the synthesized proteins. For immunoprecipitation analysis, the translation reaction mixture was diluted with 4 volumes of RIP buffer A (1% Triton X-100, 0.1% sodium desoxycholate, 0.1% sodium dodecyl sulfate [SDS], 20 mM Tris-HCl, 100 mM NaCl, 1 mM EDTA, pH 7.5) and 1 volume of 10% SDS. The mixture was heated at 95°C for 10 min, cooled on ice, and sonicated for 10 to 20 s. Thereafter, lysates were cleared by centrifugation for 1 h at 45,000 rpm in a TLA 45 rotor (Beckman), and the supernatant was saved for further analysis. The antisera used for immunoprecipitation generally were preincubated with 10 volumes of a 10% suspension of *Staphylococcus aureus* bacteria prepared as described by Kessler (23). The antibody-*S. aureus* mixture was incubated at room temperature for 1 h with periodic shaking; this was followed by two washes in RIP buffer A to remove unbound antibodies. The antibody-*S. aureus* mixture was then resuspended in RIP buffer A to give a 10% suspension, and 10 to 50 μl of this suspension was added to the pretreated in vitro translation mixture. After 1 h of shaking at room temperature, the bacteria were pelleted and the supernatant was either discarded or subjected to a second immunoprecipitation. The pelleted bacteria of the first and second immunoprecipitations were resuspended in RIP buffer A and layered on a 2-ml cushion of RIP buffer D (25% sucrose, 1% Triton X-100, 0.5% sodium desoxycholate, 0.1% SDS, 0.2% bovine serum albumin, 20 mM Tris-HCl, 100 mM NaCl, 1 mM EDTA, pH 7). The bacteria were pelleted for 15 min at 5,000 rpm at 4°C, the supernatant was removed, and the pellet was washed once with 1 ml of RIP buffer B (1% Triton X-100, 0.5% sodium desoxycholate, 0.1% SDS, 20 mM Tris-HCl, 100 mM NaCl, 1 mM EDTA, pH 7.5) and once with 1 ml of RIP buffer C (0.2% Triton X-100, 20 mM Tris-HCl, 100 mM NaCl, 1 mM EDTA, pH 7). The bound immune complexes were then eluted in sample buffer by heating for 10 min at 95°C. The *S. aureus* bacteria were removed by centrifugation, and the supernatants were analyzed on SDS-polyacrylamide gels as described previously (12, 47). After electrophoresis, the gels were processed for fluorography with En^{3}Hance as recommended by the supplier (New England Nuclear, Boston, Mass.), dried, and exposed to Kodak XAR-5 X-ray films at −70°C.

RESULTS

Generation of region-specific antisera. The strategy chosen to generate region-specific antisera involved the production of several fusion proteins encompassing different regions of the ORF1 polypeptide and the ORF2 polypeptide and the use of these proteins for immunization of rabbits. Table 1 and Fig. 1 summarize the relevant features of the plasmids that were constructed for the expression of RHDV cDNA fragments in

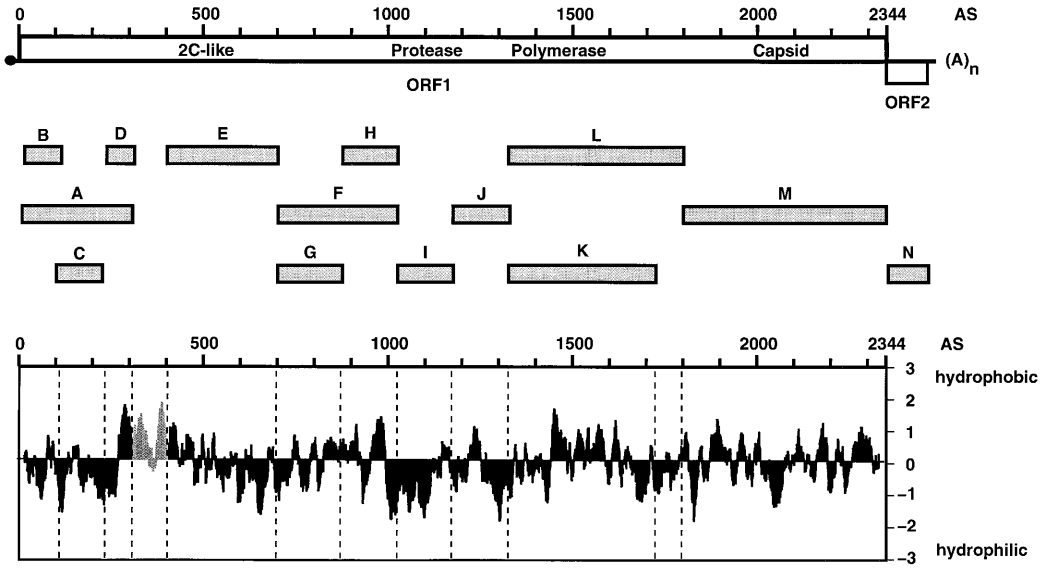

FIG. 1. Schematic representation of the RHDV genome and the cDNA fragments expressed in *E. coli*. The open reading frames ORF1 and ORF2 are indicated by bars. An amino acid scale is drawn above ORF1. The cDNA fragments A to N expressed in *E. coli* are indicated below the genome as shaded bars. The bottom part shows a hydrophilicity plot of the ORF1 polyprotein. The diagram was generated with the program PEPPLOT by using the algorithm of Kyte and Doolittle and a window size of 20 amino acids. Vertical broken lines indicate the boundaries of the polyprotein segments that are encoded by the cDNA fragments A to M. Gray shading is used to mark the part of the hydrophilicity plot corresponding to amino acids 303 to 390 of the polyprotein. This part could not be expressed in *E. coli*. AS, amino acids.

E. coli and of the fusion proteins encoded by these plasmids. In each of these plasmids, the RHDV cDNA fragment was fused in frame to the first 97 to 99 codons of the RNA polymerase gene of bacteriophage MS2; thus, each of the fusion proteins encoded by plasmids A to T comprises about 11 kDa of the MS2 polymerase in addition to the polypeptides that are specified by the RHDV cDNA fragments. Antibodies against the MS2 polypeptide could therefore be used to identify the expression products by Western blot analysis. Fusion proteins of the expected size were produced upon induction of bacteria harboring plasmids A to N, and each fusion protein was recognized by antibodies against the MS2 polymerase in Western blot analyses (data not shown). The fusion proteins appeared as insoluble aggregated material (inclusion bodies), and only a small amount of fusion protein was detected in the soluble fraction (data not shown). Highly purified fusion proteins were prepared by centrifugation of the bacterial lysate and extraction of the inclusion bodies with 7 M urea (Fig. 2). Considering expression of different parts of the ORF1 polyprotein, SDS-polyacrylamide gel electrophoresis (SDS-PAGE) analysis of the 7 M urea extract revealed an enormous variation in the fusion protein yields. The smallest amount was obtained for fusion proteins G and F.

For plasmids Q to T, fusion proteins of the expected size were not detectable in the 7 M urea extract. Western blot analyses confirmed that these proteins either were not produced or were present in very small amounts (not shown). Bacteria harboring these plasmids ceased to grow after induction, which suggested a toxic effect of the fusion proteins. Because each of the plasmids Q to T contained a short part of ORF1 from nucleotide 915 to 1185 that encodes the most hydrophobic part of the polyprotein (amino acids 303 to 390 [Fig. 1]), we suspect that this part is responsible for the toxic effect of the fusion proteins.

The fusion proteins A to N were further purified by preparative SDS-gel electrophoresis and used to immunize rabbits. The reactivities of the generated antisera were assessed by immunoprecipitation and Western blot analyses. Each of the antisera recognized its viral antigen(s), as shown below.

Location of the sequence coding for VPg. Both the genomic and subgenomic RNAs of RHDV carry a VPg of approximately 15 kDa at their 5′ ends (32). To determine the location of the coding sequence of this protein, virion RNA was labeled with radioactive iodine, and the RNA was subsequently degraded with RNase. As shown in Fig. 3, VPg was the only abundant protein in the sample (lane 11). The labeled material was subjected to immunoprecipitation with various region-spe-

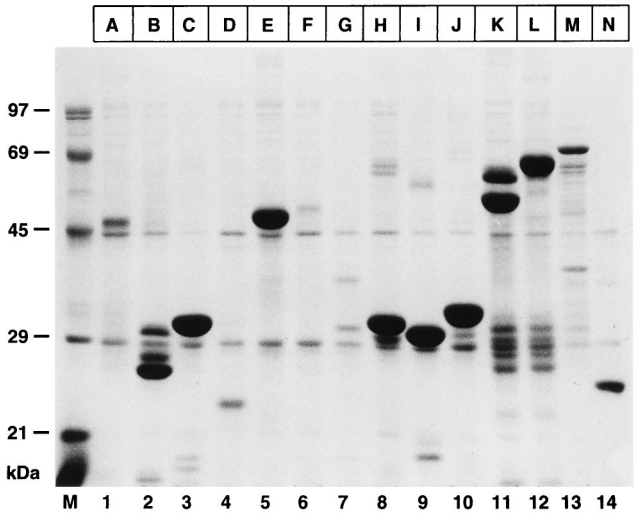

FIG. 2. SDS-PAGE analysis of fusion proteins A to N. Plasmids pEX-A to pEX-N were expressed in *E. coli*. At 2.5 h after induction, the cells were lysed and insoluble material was collected by centrifugation. The pellet was washed with 1 M urea and homogenized in 7 M urea–0.1% Tween 20. Aliquots of the 7 M urea extract were then electrophoresed in an SDS–10% polyacrylamide gel, and proteins were visualized by staining with Coomassie blue. Lane M, markers.

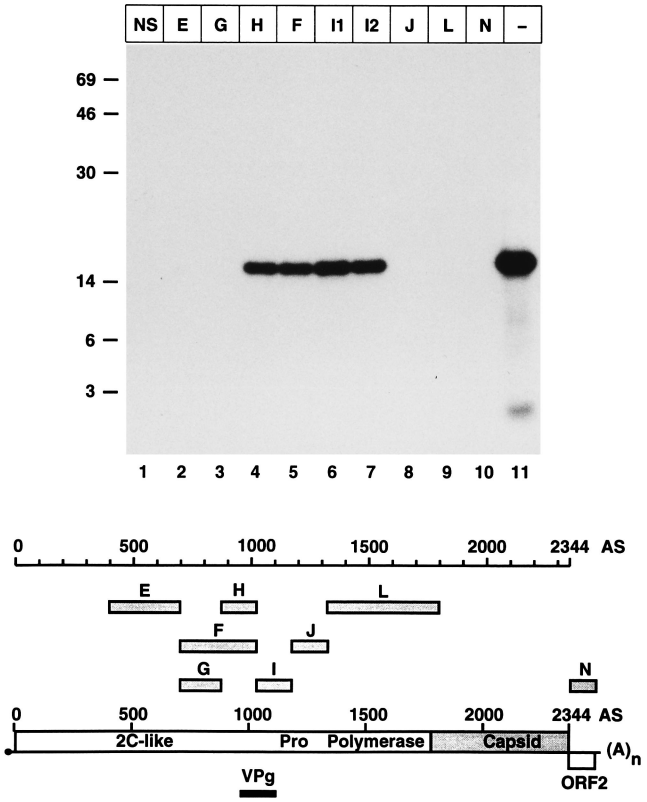

FIG. 3. Location of VPg-coding sequence. Immunoprecipitation of iodinated VPg with region-specific antisera is shown. RNA was isolated from purified virus particles and labeled with ^{125}I. The RNA was then degraded with RNase, and the radioactive material was subjected to immunoprecipitation. The RNase-digested sample (lane 11) and the immunoprecipitates (lanes 1 to 10) were electrophoresed in an SDS–12% polyacrylamide gel. Lanes I1 and I2, sera from two different rabbits which were both immunized with fusion protein I. Letters above the lanes indicate the antisera that were used for immunoprecipitation. NS, preimmune serum. A schematic diagram of the ORF1 polyprotein is shown below the gel. The position of the VPg is indicated by a black bar extending from segment H into segment I of the polyprotein. For the features of the different antisera see also Table 1.

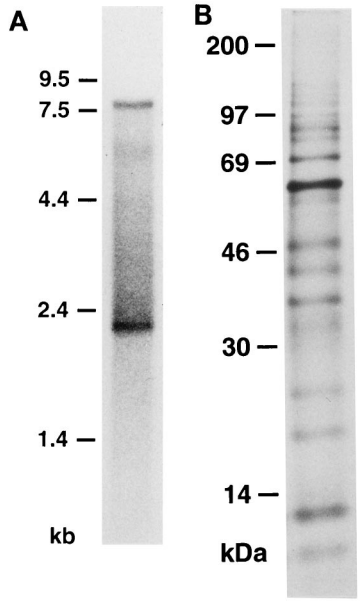

FIG. 4. Demonstration of RNA derived from RHDV virions and its in vitro translation products. (A) Northern blot with RNA isolated from gradient-purified RHDV virions hybridized against an RHDV-specific probe. The size of an RNA ladder is indicated. (B) SDS-PAGE analysis of products generated by in vitro translation of the RNA shown in panel A in the presence of [^{35}S]methionine.

cific antisera. VPg was recognized by antisera against segments F, H, and I of the polyprotein but not by antisera against segments E, G, J, L, and N (Fig. 3). This experiment showed that the VPg extends from segment H into segment I of the polyprotein.

Proteolytic processing of the ORF1 polyprotein in vitro and identification of nonstructural proteins. A tissue culture system for propagation of RHDV is not available. We therefore decided to study the proteolytic processing of the ORF1 polyprotein in vitro, using RRLs. Translation reactions were programmed with viral RNA isolated from purified viral particles. These RNA preparations contained the genomic RNA and the subgenomic RNA of RHDV (Fig. 4A). Pilot experiments confirmed our prediction that the ORF1 polyprotein of RHDV is proteolytically cleaved in the RRL, since a variety of discrete bands was detected instead of the full-length ORF1 polyprotein of about 260 kDa (Fig. 4B). To identify the cleavage products, the translation reaction mixtures were subjected to immunoprecipitation with the complete panel of region-specific antisera.

Immunoprecipitation with the anti-B serum led to the detection of one major band of 16 kDa (p16) (Fig. 5, lane 2). The same protein also reacted with the anti-A serum, which predominantly precipitated a polypeptide of 23 kDa (p23) (Fig. 5, lane 3). p23 represents the major product recognized by the anti-D serum (Fig. 5, lane 4). From these findings it was concluded that (i) p16 comprises the extreme N-terminal part of the ORF1 polyprotein and (ii) p16 most likely does not overlap p23. With regard to the molecular masses, it is probable that p23 immediately follows p16 and that the C terminus of p23 is located between segments D and E of the polyprotein. The

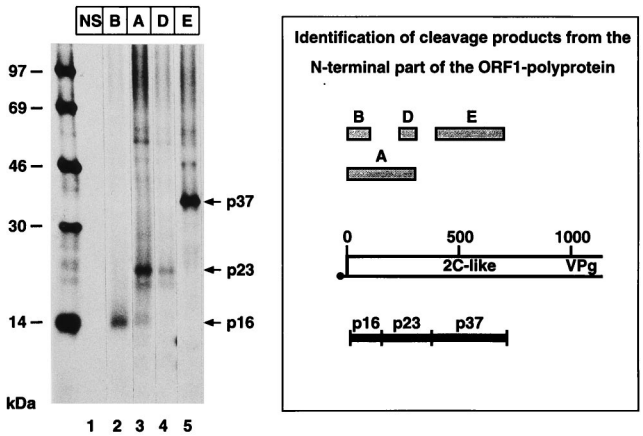

FIG. 5. Immunoprecipitation of in vitro translation products derived from the 5′ region of the RHDV RNA. RHDV RNA isolated from purified viral particles was translated in RRLs for 1 h at 30°C in the presence of [^{35}S]methionine. The translation products were identified by immunoprecipitation with the indicated region-specific antisera and SDS-PAGE analysis of the precipitated proteins. A schematic representation of the N-terminal part of the ORF1 polyprotein is shown at the right. The segments of the polyprotein that are recognized by the antisera are indicated above the polyprotein. The proteins that were precipitated by the antisera are shown as black bars below the polyprotein. The features of the antisera are summarized in Table 1.

failure to detect p23 with the anti-E serum (Fig. 5, lane 5) was consistent with this conclusion. Instead, the anti-E serum recognized a major band of 37 kDa (p37). The quantities of other bands visible in Fig. 5 varied considerably in different experiments, whereas p16, p23, and p37 were consistently detected as prominent bands. This finding indicates that these other bands probably correspond to uncleaved products encompassing two final products (i.e., bands in the range of 60 kDa) or products of internal initiation, which was always observed after in vitro translation of RHDV RNA. Taken together, the above-described data showed that the N-terminal third of the ORF1 polyprotein is processed in vitro into three major proteins of 16, 23, and 37 kDa which are arranged in the order NH_2-p16-p23-p37-. . .-COOH.

To identify the proteins derived from the central part of the polyprotein, antisera against regions F, G, H, I, and J were used (Fig. 6A). Immunoprecipitation with the anti-G serum revealed a strong band of 41 kDa, which was also detected by the anti-F, anti-H, and anti-I sera but not by the anti-J serum. This result demonstrated that p41 covers part of segment I but does not reach into segment J of the polyprotein. In addition to p41, the antisera recognized several proteins with higher molecular masses. A protein of 117 kDa (p117) was detected by all five antisera, and a protein of 87 kDa (p87) was detected by all antisera except the anti-G serum. In some lanes of Fig. 6A the latter two proteins are barely visible, because a substantial smear of translation products occurred in the high-molecular-mass range. This smear was particularly prominent in immunoprecipitations with the anti-F and anti-G sera but was also observed with other antisera. To reduce this background, a modified immunoprecipitation procedure that consisted of two sequential immunoprecipitations with different antisera was employed (Fig. 6B). Immunoprecipitation with the anti-F serum resulted again in an intense background smear that completely obscured p87 and p117, whereas p41 was still visible as a distinct band (Fig. 6B, lane 2). When two sequential immunoprecipitations were performed with anti-E as the first serum and anti-F as the second serum, both p87 and p117 were clearly visible as distinct bands (Fig. 6B, lane 3). Obviously, most of the high-molecular-mass smear was removed by the first immunoprecipitation with the anti-E serum, whereas p87 and p117 remained in the supernatant and were precipitated by the anti-F serum in the second round of immunoprecipitation. A comparison of lanes 2 and 3 of Fig. 6B revealed that the immunoprecipitation with anti-E serum also removed a 37-kDa band which was detected as a faint band by the anti-F serum in lane 2. This finding indicates that the 37-kDa band is identical to p37 described above. Taking together the results from Fig. 6A and B, the following conclusions can be drawn. (i) p41 and p117 probably possess the same N terminus, because both are recognized by the anti-G serum but not by the anti-E serum. (ii) There is probably no additional cleavage product between these proteins and the cleavage product p37, which implies that p41 immediately follows p37 in the ORF1 polyprotein. (iii) p87 lacks the N-terminal region of p41 and p117, since it is not recognized by the anti-G serum. (iv) p87 overlaps the C-terminal part of p41, since both proteins are recognized by the anti-F and anti-I sera. (v) p41 does not contain the protease and most likely ends with amino acid 1108, which represents the P1 position of a previously determined cleavage site (54). (vi) Finally, p41 contains one cleavage site and is therefore composed of two proteins. One of these proteins is represented by VPg, which extends from region H into region I of the polyprotein and covers the C-terminal third of p41 (Fig. 3). The other protein covers the N-terminal two-thirds of p41 and encompasses the region between p37 and VPg. On the

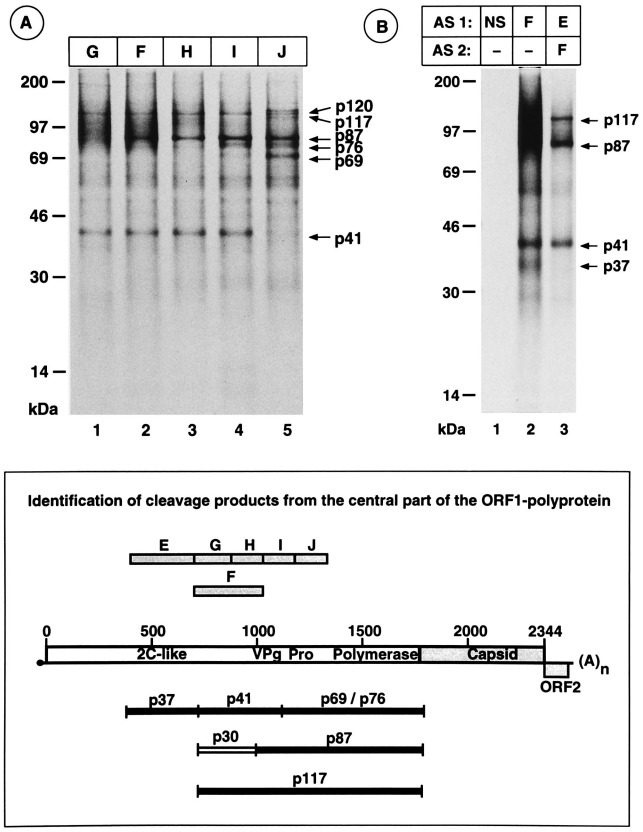

FIG. 6. Proteins encoded in the central region of the RHDV RNA. RHDV RNA isolated from purified viral particles was translated in RRLs for 1 h at 30°C in the presence of [^{35}S]methionine. The translation products were then identified by immunoprecipitation with the indicated region-specific antisera and SDS-PAGE analysis of the precipitated proteins. In one experiment the translation mixture was first subjected to immunoprecipitation with the anti-E serum, and the supernatant obtained was then subjected to immunoprecipitation with the anti-F serum (panel B, lane 3). Lane 2 in panel B shows the proteins that were recognized by the anti-F serum without prior precipitation with the anti-E serum. The dashes indicate that no second immunoprecipitation was performed. NS, preimmune serum. A schematic representation of the ORF1 polyprotein is shown below the gels. The locations of the precipitated proteins are indicated below the polyprotein, and the segments of the polyprotein that are recognized by the antisera are indicated above the polyprotein. For features of the antisera, see also Table 1. AS 1 and AS 2, antisera for the first and second precipitations, respectively.

basis of the molecular masses of p87 and p117 and assuming that both proteins have identical C termini, the postulated cleavage product that resides in the N-terminal parts of p117 and p41 has an estimated size of 30 kDa. From now on this protein will be referred to as p30. It should be noted, however, that neither p30 nor VPg was detected after in vitro translation. As shown by the formation of p87, the cleavage site at the boundary of these proteins is recognized in the RRL, suggesting that the VPg and the preceding nonstructural protein are unstable in the RRL. Protein p41 is most likely identical to the previously described p43 (1).

The data outlined above show that p41 extends to the N-terminal boundary of the protease, which is located in segment I of the polyprotein. It was therefore anticipated that the cleavage product that follows p41 should be recognized by the anti-I and anti-J sera but not by the anti-H serum. Figure 6A reveals two translation products, of 69 and 76 kDa, that satisfy these criteria. The larger protein, p76, was readily visible after immunoprecipitations with the anti-I serum, whereas the smaller

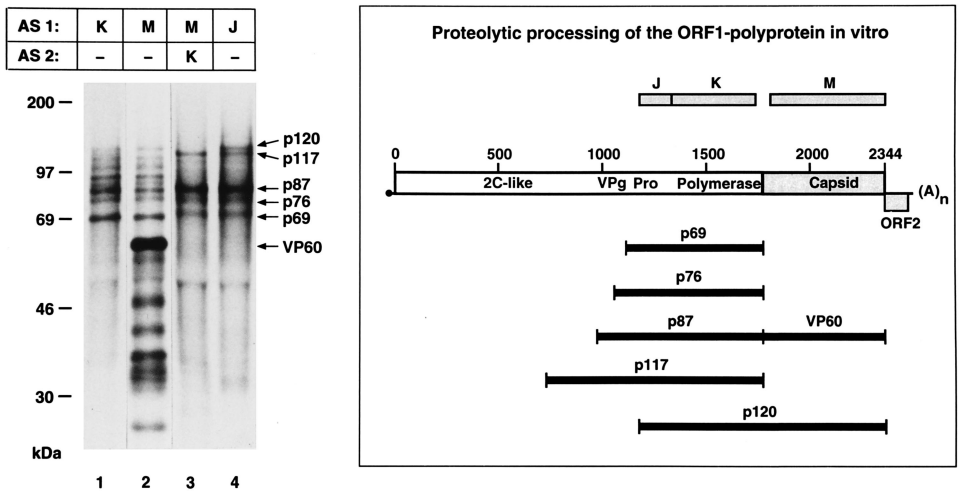

FIG. 7. Processing products derived from the 3′ half of the ORF1 polyprotein. RHDV RNA was translated in RRLs and analyzed by immunoprecipitation as described for Figs. 5 and 6. The antisera used are indicated above the gel. The right part of the figure shows a schematic representation of the ORF1 polyprotein. The segments of the polyprotein that are recognized by the antisera are indicated above the polyprotein, and the locations of the precipitated proteins are indicated below the polyprotein. AS 1 and AS 2, antisera for the first and second precipitations, respectively.

protein, p69, was barely detectable with this antiserum, suggesting that p69 is not part of segment I. Both proteins extend beyond the C terminus of the protease, which is 15 kDa in size (54), and contain at least part of the polymerase. This is also the case for the cleavage products p87, p117, and a protein of 120 kDa (p120), the largest protein recognized by the anti-J serum (Fig. 7, lane 4). Additional proteins extending into the putative polymerase were detected by the anti-K serum (Fig. 7, lane 1). Since these proteins were 68 to 120 kDa in size, which is larger than the calculated molecular mass of the polymerase (58 kDa), it was concluded that most or all of these proteins extend beyond the C terminus of the polymerase into the capsid protein. This conclusion was supported by immunoprecipitation with antiserum against fusion protein M, which covers the C-terminal 58 kDa of the ORF1 polyprotein. As expected, this antiserum precipitated a major band of 60 kDa, which corresponds to the mature capsid protein VP60 (Fig. 7, lane 2). In addition, the anti-M serum precipitated several smaller proteins; these are obviously truncated derivatives of the capsid protein, since none of them was recognized by the anti-K serum. The anti-M serum also precipitated a large number of protein species with molecular masses of between 68 and 120 kDa, which are apparently due to incomplete cleavage at the polymerase-capsid protein boundary. These proteins were also recognized by the anti-K serum, which hampered identification of translation products that are cleaved at the C-terminal boundary of the polymerase. To overcome this difficulty, sequential immunoprecipitations with the anti-M and anti-K sera were performed. In such an experiment, p69, p76, p87, and p117 were specifically recognized by the anti-K serum (Fig. 7, lane 3). From this result it was clear that these proteins do not extend into the capsid protein, since otherwise they would have been removed by the anti-M serum in the first immunoprecipitation. We therefore conclude that p69, p76, p87, and p117 are generated by a specific cleavage at the C-terminal boundary of the polymerase. It should be noted that precursors comprising the capsid protein and any of these four proteins were not observed, which indicates complete cleavage at the polymerase-VP60 boundary. This is in marked contrast to the incomplete cleavage of the translation products with molecular masses of between 68 and 120 kDa, which were detected by the anti-M serum. The results from Fig. 6 show that the anti-I serum recognized p69 but not p120. This indicates that p120 and the smaller translation products, which extend from the polymerase into the capsid protein, do not include the complete protease. Accordingly, cleavage at the polymerase-VP60 boundary appears to be incomplete only for precursors that lack an active protease. Since previous studies have shown that the TCP is responsible for cleavage at the polymerase-VP60 boundary (5, 54), our data imply that at least in vitro this cleavage occurs predominantly in *cis* and is rather inefficient in *trans*. Our data also indicate inefficient cleavage at the protease-polymerase boundary, since neither the mature protease nor the mature polymerase was detected by the anti-J and anti-K sera. This finding is in agreement with our previous data which showed that the protease-polymerase boundary appears to be resistant to cleavage in vitro and is cleaved very inefficiently in *E. coli* (5, 54).

As discussed above, the 69-kDa protein is the smallest protein recognized by the anti-K and anti-J sera and also appears to be the smallest protein that includes the complete protease and the complete polymerase. From this finding it can be concluded that p69 most likely represents the cleavage product that covers the region between p41 and the capsid protein VP60 and thus is equivalent to the previously identified p73 (1). In contrast to p69, p76 probably extends beyond the N terminus of the protease into VPg and is most likely due to internal initiation. Internal initiation probably also accounts for the additional translation products, whose N termini are located within or downstream of the protease and which are not cleaved at the polymerase-VP60 boundary.

Genetic map of ORF1. The data from the in vitro translation study are summarized in Fig. 8, which assigns the products generated by in vitro cleavage of the ORF1 polyprotein to their coding sequences in the genome. The map reveals a total of seven cleavage sites, which are cleaved in vitro to different extents. At sites 1 and 3 cleavage appears to be complete as indicated by the absence of uncleaved precursor proteins that encompass the flanking cleavage products. Cleavage between the putative polymerase and the capsid protein VP60 (site 7) is also complete, taking into account that the observed uncleaved proteins are most likely aberrant products due to internal ini-

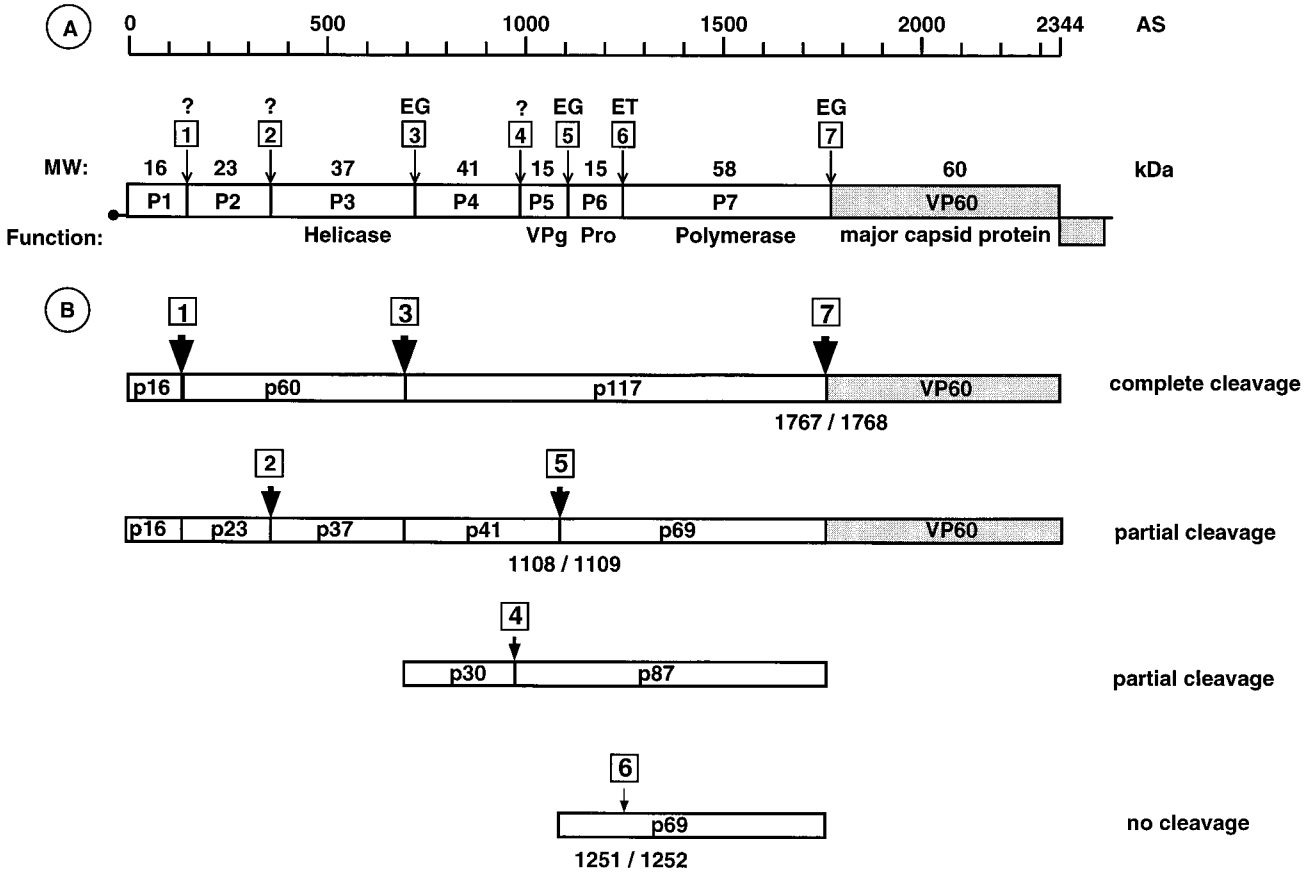

FIG. 8. Schematic representation of the in vitro cleavage products of the ORF1 polyprotein and proposed genetic map of ORF1. (A) The genomic RNA of RHDV is represented below the scale bar. Open reading frames are shown as open or shaded bars. Cleavage sites in the ORF1 polyprotein are indicated by vertical lines and numbered 1 to 7. The nonstructural proteins are designated P1 to P7. The molecular masses of the proteins (in kilodaltons) are shown above the bars, and their established or putative functions are indicated below the bars. Protein p60 was detected in several experiments but is difficult to see in Fig. 5. P4 (p41) is equivalent to a protein of 43 kDa described before (1). Cleavage sites 3, 5, 6, and 7 have been determined by N-terminal sequencing of the respective proteins or in vitro mutagenesis experiments (1, 54). Cleavage sites equivalent to sites 3 and 4 were also determined for the human calicivirus Southampton virus (29). (B) Schematic representation of the cleavage products of the ORF1 polyprotein observed in the RRL.

tiation. The in vitro assays revealed partial cleavage at sites 4 and 5 and no cleavage at site 6. In addition, several experiments indicated incomplete cleavage at site 2, since polypeptides of about 60 kDa which reacted with antisera against segments A, C, D, and E, but not B, were detected (see also Fig. 5). Although these results might in part be due to limitations of the in vitro system, it is reasonable to assume that the large variation in cleavage efficiency at the different cleavage sites reflects a mechanism by which the amount of distinct functional proteins is regulated during the viral life cycle.

The seven cleavage sites identified so far in the ORF1 polyprotein define the boundaries of eight putative final cleavage products. In our study four of these cleavage products were observed in vitro (p16, p23, p37, and VP60), whereas the remaining proteins (p30, VPg, TCP, and pol) were detected only as parts of larger proteins that are composed of two (p41 = p30 + VPg, p69 = TCP + pol), three (p87 = VPg + TCP + pol), or four (p117 = p41 + p69) of the postulated end products. Because of the limitations of our in vitro system, pulse-chase studies could not be performed. It is therefore presently unclear if the larger proteins are actually precursors that are further cleaved or if they represent stable end products. Proper cleavage of these proteins may require the presence of cellular cofactors that are lacking in the in vitro system. The failure to detect the final cleavage products may also be due to proteolytic degradation of these proteins.

The ORF2 product represents a structural protein. Viral particles were purified from a liver homogenate of an infected rabbit and subjected to Western blot analyses with region-specific antisera to examine if the virions contain viral proteins in addition to the capsid protein VP60. As expected, the anti-M and the anti-L sera showed a strong reaction with VP60 (Fig. 9). These antisera also detected smaller proteins that are commonly observed in immunoblots of RHDV particles and are probably due to proteolytic degradation of the capsid protein. No specific signal was obtained with antisera against those regions of the ORF1 polyprotein that precede the capsid protein, indicating that the proteins derived from this part of the polyprotein are nonstructural proteins or, like VPg, are present in very small amounts. In contrast, both of the anti-N sera showed a specific reaction with a protein of approximately 10 kDa. This finding indicated that the ORF2 polypeptide or a cleavage product of this protein represents a component of RHDV virions. The signal of the 10-kDa protein was much weaker than the signal of the capsid protein VP60 obtained with the anti-M serum, suggesting that the 10-kDa protein was present in a smaller amount than VP60. These results could be verified by immunoprecipitation experiments with extracts prepared after iodine labeling of purified virions. In addition to VP60, VP10 and VPg were detected. The latter two proteins were present in much smaller amounts than VP60 (data not shown). In conclusion, the analyses show that a minor capsid

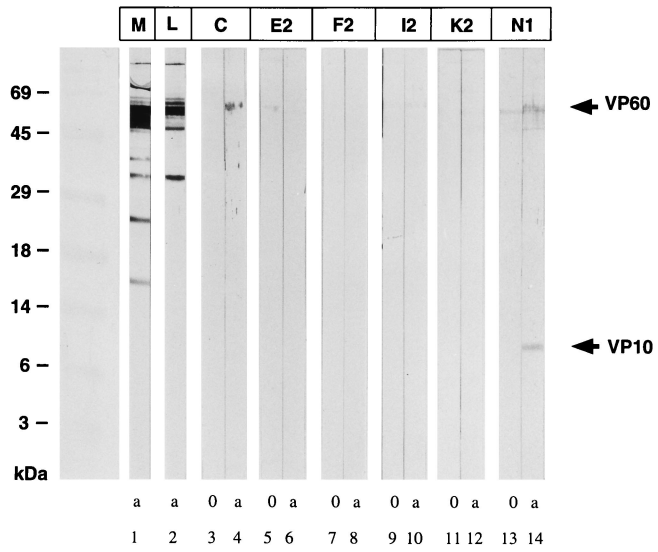

FIG. 9. Immunoblot of purified viral particles of RHDV with region-specific antisera. Purified RHDV particles were electrophoresed in SDS–12% polyacrylamide gels and analyzed by immunoblotting with the indicated region-specific antisera. Numbers are used to distinguish between sera from different rabbits. The rabbit sera were used at a dilution of 1:200. Abbreviations: a, antiserum; 0, preimmune serum. Because of the large amount of VP60 present on the blot, some of the sera show a nonspecific reaction with this protein. The features of the antisera are summarized in Table 1.

protein of approximately 10 kDa is encoded in ORF2. Furthermore, these analyses establish that VP60 and VPg are the only structural proteins encoded in ORF1.

DISCUSSION

Sequence comparisons have shown that caliciviruses are related to members of the picornavirus-like superfamily of plus-stranded RNA viruses (31, 36). This finding is confirmed and extended in our present study, which reveals a remarkable similarity in genome organization between RHDV and picornaviruses (Fig. 10). According to the results of our in vitro studies, RHDV, like picornaviruses, encodes six nonstructural proteins and VPg as parts of one large polyprotein. The nonstructural proteins include a putative RNA helicase, a TCP, and an RNA polymerase that are conserved in all members of the picornavirus-like superfamily of plus-stranded RNA viruses (11, 15, 24). In the ORF1 polyprotein of RHDV, these proteins are arranged in an order that is common to all members of the picornavirus superfamily, namely, helicase-VPg-TCP-polymerase (Fig. 10). Our data also show that RHDV encodes an additional nonstructural protein that is located between the helicase and VPg and is analogous in location to the 3A protein of poliovirus and a protein of 6 kDa encoded by potyviruses (44, 45). The N-terminal part of the ORF1 polyprotein of RHDV that precedes the putative helicase comprises the remaining two nonstructural proteins of RHDV, p16 and p23. These proteins are analogous in location to the 2A and 2B proteins of picornaviruses. Thus, each of the nonstructural proteins encoded by all picornaviruses has its counterpart in the ORF1 polyprotein of RHDV.

Previous studies showed that the TCP of RHDV is similar in function to the picornaviral 3C protease (5, 54). Although functional studies have not yet been performed for the other nonstructural proteins, the extensive sequence similarities between the putative RNA helicase 2C of picornaviruses and the nonstructural protein p37 of RHDV indicates that these proteins have a similar role in genome replication. The same argument applies to the 3D polymerase protein of picornaviruses and the RHDV RNA polymerase, the putative cleavage product p58 which constitutes the C-terminal part of the TCP-pol precursor p69. Functional homology is also obvious in the case of VPg. In picornaviruses this protein or its precursor 3AB has been proposed to serve as a primer for the viral polymerase during initiation of positive-strand RNA synthesis (14, 26, 41–43). This could also be the case for the VPgs of RHDV and other caliciviruses. It has to be stressed, however, that calicivirus VPgs are almost five times the size of picornavirus VPgs, whereas the putative helicases and RNA polymerases of RHDV and picornaviruses are very similar in size. This finding suggests that the calicivirus VPgs have additional functions that are not shared by their picornavirus counterparts. One of these functions might be to play a role in translation initiation, a process which obviously differs for calici- and picornaviruses.

While the putative helicase, the putative RNA polymerase, and, to a lesser extent, the TCP have significant sequence homology with the corresponding picornavirus proteins, this is not the case for the nonstructural proteins p23 and p30. However, our studies reveal a similar behavior of these proteins and their picornavirus counterparts in *E. coli*; like 2B and 3A of poliovirus, both p23 and p30 appear to be toxic. In contrast, the other nonstructural proteins of RHDV and poliovirus, including the trypsin-like proteases, exhibit no or only a modest toxic effect in *E. coli* (25). The toxicity of the 2B and 3A proteins of poliovirus was attributed to amphipathic helices, which are thought to interact with the bacterial membrane. Computer analysis of the ORF1 polypeptide of RHDV showed the presence of similar amphipathic helices in the N- and C-terminal parts of p23 and the amino-terminal half of p30 (data not shown). Although at present the existence of the amphipathic helices is still hypothetical for both the poliovirus polyprotein and the ORF1 polyprotein of RHDV, our results suggest that the nonstructural proteins p23 and p30 have structural and maybe also functional similarities with 2B and 3A of picornaviruses.

The extreme N-terminal part of the ORF1 polyprotein of RHDV contains a nonstructural protein of 16 kDa (p16) that occupies a position in the polyprotein analogous to the 2A protein of picornaviruses. Like p23 and p30, the nonstructural protein p16 shows no obvious sequence similarity with its picornavirus-counterpart. This is not surprising, since in picornaviruses the 2A protein is one of the most variable nonstructural proteins with regard to size and sequence. In foot-and-mouth disease virus and enteroviruses, 2A exhibits proteolytic activity and mediates proteolytic cleavage at its own N or C terminus (43). However, while in enteroviruses the 2A protease belongs to the trypsin-like family of proteases, the 2A protein of foot-and-mouth disease virus appears to be only 16 amino acids in length and shows no significant similarity to any known protease family (46). Sequence analysis of the nonstructural protein p16 did not reveal the presence of a catalytic triad typical of trypsin-like proteases. In many viral polyproteins, papain-like proteases constitute the first polypeptide (13, 16), but p16 also shows no homology to these proteases. A low level of similarity between the C-terminal part of p16 and the 2A protein of foot-and-mouth disease virus was apparent (data not shown). Preliminary studies indicated that the N-terminal half of the ORF1 polyprotein of RHDV contains no protease. Thus, our data suggest that the nonstructural protein p16, like the 2A protein of hepatitis A virus, has no proteolytic activity, which implies that all cleavages in the viral polyprotein might be executed by the 3C-like TCP (48, 49). For poliovirus, experimental evidence which indicates a multifunctional role of

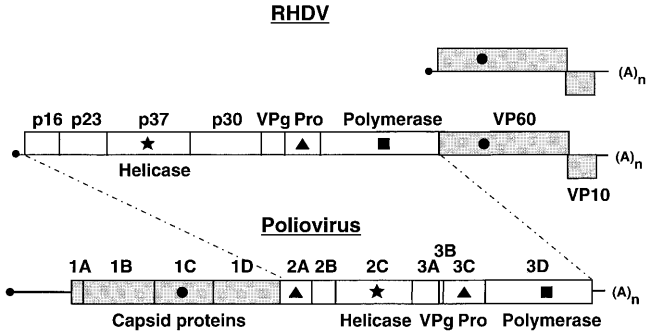

FIG. 10. Genetic map of RHDV in comparison with poliovirus. Schematic representations of the RHDV and poliovirus RNAs are shown, with noncoding regions shown as solid lines, coding regions drawn as bars, and VPgs indicated as small black circles. Nonstructural proteins are represented by open bars, and structural proteins are represented by shaded bars. Conserved amino acid sequences are indicated: ★, nucleotide-binding motif; ▲, cysteine protease; ■, polymerase domain; ●, region of VP60 homologous to 1C (VP3) of poliovirus.

the 2A protein in the replication cycle has been reported (18, 30, 34, 43). Some studies also suggest that the proteolytic activity of the 2A protein is dispensable for some of these functions (3). In view of these findings, it will be an interesting task for future studies to determine if the picornavirus 2A proteins and the amino-terminal cleavage product of the calicivirus polyprotein share a nonproteolytic function.

Our results concerning processing of the N-terminal part of the RHDV polyprotein differ considerably from the data published by Alonso and coworkers (1). Those authors found a protein of 80 kDa which probably encompasses the three processing products p16, p23, and p37 identified in the present study. The reason for this discrepancy is presently not known. For Southampton virus, a 41-kDa protein corresponding to p37 was identified, indicating that the amino-terminal part of the polyprotein of this calicivirus is processed in vitro (29). However, the same authors did not detect polypeptides corresponding to p16 or p23. Instead, a protein of 48 kDa was found, which again is apparently not further processed in vitro. Like RHDV, the human caliciviruses cannot be propagated in tissue culture, and further processing of p48 might occur within infected cells.

Cleavage of the poliovirus polyprotein gives rise to several long-lived precursor proteins that are only partially cleaved. Interestingly, some of these precursors composed of two final cleavage products are analogous to some cleavage products generated in vitro from the ORF1 polyprotein of RHDV. Most notable among these precursors are the 2BC, 3AB, and 3CD proteins of poliovirus, which correspond to the cleavage products p60, p41, and p69 of RHDV, respectively. Since each of the poliovirus precursors (3AB and 3CD [2, 14, 19, 20, 26, 33, 41, 42, 55] and 2BC [4, 9]) either has been shown or is presumed to have a functional role in genome replication distinct from its final products, it is interesting that the analogous fusion proteins are generated from the ORF1 polyprotein of RHDV, even though interpretation of these data has to take into account the limitations of the in vitro system.

A common feature of all caliciviruses is the existence of a small open reading frame of 300 to 600 nucleotides in length that overlaps the gene of the major capsid protein and extends close to the 3′ end of the genomic RNA (7, 8, 22, 27, 31, 37). Our results show that a capsid protein of approximately 10 kDa (VP10) is encoded in the respective open reading frame (ORF2) of RHDV. This protein was also observed after in vitro translation of RHDV virion RNA (data not shown). Interestingly, the apparent molecular mass of this basic protein is considerably lower than the calculated molecular mass of the ORF2 polypeptide (12.7 kDa). It is presently unclear whether this is due to either its amino acid composition or proteolytic cleavage of the primary translation product. In a recent study, the corresponding ORF3-encoded polypeptide of FCV has been identified in FCV-infected cells (21). Like VP10 of RHDV, this protein has an apparent molecular mass considerably lower than the calculated molecular mass of the ORF3-encoded polypeptide. Although VP10 was identified as a virion component for the first time in the present study, it is highly likely that the corresponding proteins of other caliciviruses also represent structural proteins. The function of the ORF2 polypeptide is not yet known, but it is intriguing that, according to our data for RHDV, this protein appears to be present in viral particles in substoichiometric amounts compared with the capsid protein VP60. Recently, it was shown that VP60 alone is able to assemble into virus-like empty particles that are indistinguishable from those which are found in livers of RHDV-infected animals (28, 35, 50). Considering these findings, we propose that VP10 could interact with both the major capsid protein VP60 and the viral RNA, thereby mediating specific encapsidation of the viral genome.

Within the picornavirus superfamily, caliciviruses are the only members which produce a subgenomic RNA. At least for RHDV, this RNA is efficiently packaged into virions, which is not a general feature of viral subgenomic RNAs. Furthermore, minus-strand copies of the subgenomic RNA have been detected in FCV-infected cells, suggesting that the subgenomic RNA is replicated like the genomic RNA (6). Taken together, these data indicate that the subgenomic RNAs of caliciviruses exhibit basic properties of a genome segment, namely, encapsidation and replication. Previous studies have demonstrated that RHDV makes use of two mechanisms to synthesize the capsid protein VP60 (5, 39, 50, 54). The first mechanism involves translation of the genomic RNA, which generates a precursor protein that is cleaved at the N-terminal boundary of the capsid protein. This translation strategy resembles those of picorna-, poty-, and sequiviruses, which are members of the picornavirus superfamily with monopartite genomes. Like RHDV, these viruses encode the capsid and the nonstructural proteins in a single open reading frame (11, 24, 45). The other expression mechanism, which is common to all caliciviruses, involves translation of the subgenomic RNA. This mechanism resembles the expression strategy of como- and nepoviruses, whose genomes are composed of two RNA molecules. The larger RNA (RNA 1) encodes the nonstructural proteins, whereas the smaller one (RNA 2) serves as mRNA for the capsid proteins. Considering their peculiar features, the subgenomic RNAs of caliciviruses can be regarded as additional genome segments that are used to express the structural proteins and in this respect represent the functional equivalent of the RNA 2 of como- and nepoviruses. Thus, the strategy of RHDV to express the major capsid protein can be best described as a unique combination of two known expression mechanisms that are used by other members of the picornavirus superfamily. These conclusions support the idea that caliciviruses or an ancestor with a similar genome organization and expression strategy constitute an evolutionary link between the two groups of viruses of the picornavirus superfamily with mono- or bipartite genomes.

ACKNOWLEDGMENTS

This work was supported by grants Th 298/3-1 and Me 1367/1-2 from the Deutsche Forschungsgemeinschaft.

REFERENCES

1. **Alonso, J. M., R. Casais, J. A. Boga, and F. Parra.** 1996. Processing of rabbit hemorrhagic disease virus polyprotein. J. Virol. **70:**1261–1265.
2. **Andino, R., G. E. Rieckhof, P. L. Achacoso, and D. Baltimore.** 1993. Poliovirus RNA synthesis utilizes an RNP complex formed around the 5′-end of viral RNA. EMBO J. **12:**3587–3598.
3. **Ansardi, D. C., R. Pal-Ghosh, D. Porter, and C. D. Morrow.** 1995. Encapsidation and serial passage of a poliovirus replicon which expresses an inactive 2A proteinase. J. Virol. **69:**1359–1366.
4. **Barco, A., and L. Carraso.** 1995. A human virus protein, poliovirus protein 2BC, induces membrane proliferation and blocks the exocytic pathway in the yeast Saccharomyces cerevisiae. EMBO J. **14:**3349–3364.
5. **Boniotti, B., C. Wirblich, M. Sibilia, G. Meyers, H.-J. Thiel, and C. Rossi.** 1994. Identification and characterization of a 3C-like protease from rabbit hemorrhagic disease virus, a calicivirus. J. Virol. **68:**6487–6495.
6. **Carter, M. J.** 1990. Transcription of feline calicivirus RNA. Arch. Virol. **114:**143–152.
7. **Carter, M. J.** 1994. Genomic organization and expression of astroviruses and caliciviruses. Arch. Virol. **9**(Suppl.)**:**429–439.
8. **Carter, M. J., I. D. Milton, P. C. Turner, J. Meanger, M. Bennett, and R. Gaskell.** 1992. Identification and sequence determination of the capsid protein gene of feline calicivirus. Arch. Virol. **122:**223–235.
9. **Cho, M. W., N. Teterina, D. Egger, K. Bienz, and E. Ehrenfeld.** 1994. Membrane rearrangement and vesicle induction by recombinant poliovirus 2C and 2BC in human cells. Virology **202:**129–145.
10. **Cubbit, D., D. W. Bradley, M. J. Carter, S. Chiba, M. K. Estes, L. J. Saif, F. L. Schaffer, A. W. Smith, M. J. Studdert, and H.-J. Thiel.** 1995. Family Caliciviridae. Arch. Virol. **10**(Suppl.)**:**359–363.
11. **Dolja, V. V., and J. C. Carrington.** 1992. Evolution of positive-strand RNA viruses. Semin. Virol. **3:**315–326.
12. **Doucet, J.-P., and J.-M. Trifaro.** 1988. A discontinuous and highly porous sodium dodecyl sulfate-polyacrylamide slab gel system of high resolution. Anal. Biochem. **168:**265–271.
13. **Dougherty, W. G., and B. L. Semler.** 1993. Expression of virus-encoded proteinases: functional and structural similarities with cellular enzymes. Microbiol. Rev. **57:**781–822.
14. **Giachetti, C., and B. L. Semler.** 1991. Role of a viral membrane polypeptide in strand-specific initiation of poliovirus RNA synthesis. J. Virol. **65:**2648–2654.
15. **Goldbach, R., and J. Wellink.** 1988. Evolution of plus-strand RNA viruses. Intervirology **29:**260–267.
16. **Gorbalenya, A. E., E. V. Koonin, and M. M. C. Lai.** 1989. Putative papain-related thiol proteases of positive-strand RNA viruses. FEBS Lett. **288:**201–205.
17. **Greenwood, F. C., W. M. Hunter, and J. S. Glover.** 1963. The preparation of ^{131}I-labelled human growth hormone of high specific radioactivity. Biochem. J. **89:**114–123.
18. **Hambidge, S. J., and P. Sarnow.** 1992. Translational enhancement of the poliovirus 5′ noncoding region mediated by virus-encoded polypeptide 2A. Proc. Natl. Acad. Sci. USA **89:**10272–10276.
19. **Harris, K. S., S. R. Reddigari, M. J. H. Nicklin, T. Hämmerle, and E. Wimmer.** 1992. Purification and characterization of poliovirus polypeptide 3CD, a proteinase and a precursor for RNA polymerase. J. Virol. **66:**7481–7489.
20. **Harris, K. S., W. Xiang, L. Alexander, W. S. Lane, A. V. Paul, and E. Wimmer.** 1994. Interaction of poliovirus polypeptide 3CD^{pro} with the 5′ and 3′ termini of the poliovirus genome. J. Biol. Chem. **269:**27004–27014.
21. **Herbert, T. P., I. Brierley, and T. D. K. Brown.** 1996. Detection of the ORF3 polypeptide of feline calicivirus in infected cells and evidence for its expression from a single, functionally bicistronic subgenomic mRNA. J. Gen. Virol. **77:**123–127.
22. **Jiang, X., M. Wang, K. Wang, and M. K. Estes.** 1993. Sequence and genomic organization of Norwalk virus. Virology **195:**51–61.
23. **Kessler, S. W.** 1975. Rapid isolation of antigens from cells with a staphylococcal protein A-antibody adsorbent: parameters of the interaction of antibody-antigen complexes with protein A. J. Immunol. **115:**1617–1624.
24. **King, A. M. Q., G. P. Lomonossoff, and M. D. Ryan.** 1991. Picornaviruses and their relatives in the plant kingdom. Semin. Virol. **2:**11–17.
25. **Lama, J., and L. Carrasco.** 1992. Expression of poliovirus nonstructural proteins in Escherichia coli cells. J. Biol. Chem. **267:**15932–15937.
26. **Lama, J., A. V. Paul, K. S. Harris, and E. Wimmer.** 1994. Properties of purified recombinant poliovirus protein 3AB as substrate for viral proteinases and as co-factor for viral polymerase 3D^{pol}. J. Biol. Chem. **269:**66–70.
27. **Lambden, P. R., E. O. Caul, C. R. Ashley, and I. N. Clarke.** 1993. Sequence and genome organization of a human small round-structured (Norwalk-like) virus. Science **259:**516–519.
28. **Laurent, S., J.-F. Vautherot, M.-F. Madelaine, G. Le Gall, and D. Rasschaert.** 1994. Recombinant rabbit hemorrhagic disease virus capsid protein expressed in baculovirus self-assembles into viruslike particles and induces protection. J. Virol. **68:**6794–6798.
29. **Liu, B., I. N. Clarke, and P. R. Lambden.** 1996. Polyprotein processing in Southampton virus: identification of 3C-like protease cleavage sites by in vitro mutagenesis. J. Virol. **70:**2605–2610.
30. **Macadam, A. J., G. Ferguson, T. Fleming, D. M. Stone, J. W. Almond, and P. D. Minor.** 1994. Role for poliovirus protease 2A in cap independent translation. EMBO J. **13:**924–927.
31. **Meyers, G., C. Wirblich, and H.-J. Thiel.** 1991. Rabbit hemorrhagic disease virus. Molecular cloning and nucleotide sequencing of a calicivirus genome. Virology **184:**664–676.
32. **Meyers, G., C. Wirblich, and H.-J. Thiel.** 1991. Genomic and subgenomic RNAs of rabbit hemorrhagic disease virus are both protein-linked and packaged into particles. Virology **184:**677–689.
33. **Molla, A., K. S. Harris, A. V. Paul, S. H. Sin, J. Mugavero, and E. Wimmer.** 1994. Stimulation of poliovirus proteinase 3C^{pro}-related proteolysis by the genome-linked protein VPg and its precursor 3AB. J. Biol. Chem. **269:**27015–27020.
34. **Molla, A., A. V. Paul, M. Schnid, S. K. Jang, and E. Wimmer.** 1993. Studies on dicistronic polioviruses implicate viral proteinase 2A^{pro} in RNA replication. Virology **196:**739–747.
35. **Nagesha, H. S., L. F. Wang, A. D. Hyatt, C. J. Morissy, C. Lenghaus, and H. A. Westbury.** 1995. Self-assembly, antigenicity, and immunogenicity of the rabbit haemorrhagic disease virus (Czechoslovakian strain V-351) capsid protein expressed in baculovirus. Arch. Virol. **140:**1095–1108.
36. **Neill, J. D.** 1990. Nucleotide sequence of a region of the feline calicivirus genome that encodes picornavirus-like RNA-dependent RNA polymerase, cysteine protease and 2C polypeptides. Virus Res. **17:**145–160.
37. **Neill, J. D., I. M. Reardon, and R. L. Heinrikson.** 1991. Nucleotide sequence and expression of the capsid protein gene of feline calicivirus. J. Virol. **65:**5440–5447.
38. **Ohlinger, V. F., B. Haas, G. Meyers, F. Weiland, and H.-J. Thiel.** 1990. Identification and characterization of the virus causing rabbit hemorrhagic disease. J. Virol. **64:**3331–3336.
39. **Parra, F., A. J. Boga, M. S. Marin, and R. Casais.** 1993. The amino terminal sequence of VP60 from rabbit hemorrhagic disease virus supports its putative subgenomic origin. Virus Res. **27:**219–228.
40. **Parra, F., and M. Prieto.** 1990. Purification and characterization of a calicivirus as the causative agent of a lethal hemorrhagic disease in rabbits. J. Virol. **64:**4013–4015.
41. **Paul, A. V., A. Molla, and E. Wimmer.** 1994. Studies with poliovirus polymerase 3D^{pol}: stimulation of poly(U) synthesis in vitro by purified poliovirus protein 3AB. J. Biol. Chem. **269:**29173–29181.
42. **Plotch, S. J., and O. Palant.** 1995. Poliovirus protein 3AB forms a complex with and stimulates the activity of the viral RNA polymerase, 3D^{pol}. J. Virol. **69:**7169–7179.
43. **Porter, A. G.** 1993. Picornavirus nonstructural proteins: emerging roles in virus replication and inhibition of host cell functions. J. Virol. **67:**6917–6921.
44. **Restrepo-Hartwig, M. A., and J. C. Carrington.** 1994. The tobacco etch potyvirus 6-kilodalton protein is membrane associated and involved in viral replication. J. Virol. **68:**2388–2397.
45. **Riechmann, J. L., S. Lain, and J. A. Garcia.** 1992. Highlights and prospects of potyvirus molecular biology. J. Gen. Virol. **73:**1–16.
46. **Ryan, M. D., and J. Drew.** 1994. Foot-and-mouth disease virus 2A oligopeptide mediated cleavage of an artificial polyprotein. EMBO J. **13:**928–933.
47. **Schägger, H., and G. von Jagow.** 1987. Tricine-sodium dodecyl sulfate-polyacrylamide gel electrophoresis for the separation of proteins in the range from 1-100 kDa. Anal. Biochem. **166:**368–379.
48. **Schultheiss, T., Y. Y. Kusov, and V. Gauss-Müller.** 1994. Proteinase 3C of hepatitis A virus (HAV) cleaves the HAV polyprotein P2-P3 at all sites including VP1/2A and 2A/2B. Virology **198:**275–281.
49. **Schultheiss, T., W. Sommergruber, Y. Kusov, and V. Gauss-Müller.** 1995. Cleavage specificity of purified recombinant hepatitis A virus 3C proteinase on natural substrates. J. Virol. **69:**1727–1733.
50. **Sibilia, M., M. B. Boniotti, P. Angoscini, L. Capucci, and C. Rossi.** 1995. Two independent pathways of expression lead to self-assembly of the rabbit hemorrhagic disease virus capsid protein. J. Virol. **69:**5812–5815.
51. **Smid, B., L. Valicek, J. Stepanek, E. Jurak, and L. Rodak.** 1989. Experimental transmission and electron microscopic demonstration of the virus of haemorrhagic disease of rabbits in Czechoslovakia. J. Vet. Med. B **36:**237–240.
52. **Strebel, K., E. Beck, K. Strohmaier, and H. Schaller.** 1986. Characterization of foot-and-mouth disease virus gene products with antisera against bacterially synthesized fusion proteins. J. Virol. **57:**983–991.
53. **Wirblich, C., G. Meyers, V. F. Ohlinger, L. Capucci, U. Eskens, B. Haas, and H.-J. Thiel.** 1994. European brown hare syndrome virus: relationship to rabbit hemorrhagic disease virus and other caliciviruses. J. Virol. **68:**5164–5173.
54. **Wirblich, C., M. Sibilia, M. B. Boniotti, C. Rossi, H.-J. Thiel, and G. Meyers.** 1995. 3C-like protease of rabbit hemorrhagic disease virus: identification of cleavage sites in the ORF1 polyprotein and analysis of cleavage specificity. J. Virol. **69:**7159–7168.
55. **Xiang, W., K. S. Harris, L. Alexander, and E. Wimmer.** 1995. Interaction between the 5′-terminal cloverleaf and 3AB/3CD^{pro} of poliovirus is essential for RNA replication. J. Virol. **69:**3658–3667.